# Chapter 4 Optimization of the Locations of the Actuators and Sensors and Active Control of Sound in the Test System

The goal of this chapter is to compare the Active Noise Control results obtained experimentally with those obtained with the finite element model. Because the location of the actuators and sensors was optimized using a genetic algorithm based on ANC results obtained with the structural-acoustic finite element model, it is of paramount importance that the model be able to provide an accurate representation of the experimental results. In the first section of this chapter, active noise control results, experimentally obtained, are compared with those obtained with the simulation. In the second part, the issues regarding the genetic algorithm are discussed, and the optimization results are presented. Finally, in the third part, control of harmonic and broad band disturbances is performed using the optimized configuration of the actuators and error sensors.

## 4.1 Active Noise Control Simulation

### *4.1.1 Experimental Set-Up*

The active system was based upon a multi-channel filtered-X LMS Algorithm (detailed in chapter 2.3). It was implemented on a Texas Instrument quad C-40 board residing in a PC. This system has been previously used in different configurations for the control of harmonic and band limited random disturbances. The set-up presented in Figure 4.1 remained the same for all configurations, although the number of error sensors was varied. Figure 4.1 shows a side and a top view of the cavity, plus a block diagram of the controller. The red dots show the positions of

the error sensors, while the control actuators are shown in green. The signal conditioning of the control, error, and reference signals is shown below these figures. In its largest configuration, the controller is operated with one reference signal, six error sensors, and four control actuators, but has also been operated with four error sensors. In the latter case, sensors 5 and 6 in Figure 4.1 were not used. Error sensors 1 to 4 have been located at the positions of the head of the passengers and driver. Error sensor 5 has been located in the middle of the cavity for global control. Error sensor 6 has been located in a corner of the cavity close to the driver because no node of pressure is located at this position. The error sensors are high-pass filtered above 40 Hz before they are input into the controller. Low-pass filtering is applied to the control signals to remove the zero-order hold effect of the D/A converter. The reference signal is the non-amplified band-pass filtered signal received by the disturbance shaker.

Three volumes have been defined in the cavity, and each of them is weighted according to its importance for the control. The upper front represents the volume ($V_1$) where control is the most important (heads of the supposed passengers). Therefore, a weight of four is applied to this volume. The lower back volume ($V_2$) is of less importance (trunk), and a weight of one is applied to this volume. A weight of two is applied to the rest of the cavity ($V_3$). The scanning system described in Figure 3.3 is used to monitor the effect of control through the cavity. In order to differentiate the three volumes, the traverse is manually moved from the back to the front of the structure with a regular step of 20 cm, except for the first three positions located at the back of the cavity, where the step is 40 cm. The weights are used in the computation of a 'pseudo' potential energy. The pseudo potential energy Ep is defined as the sum of the pressure squared at the sensors, as:

$$E_p = 4\sum_{V_1} P_i^2 + 2\sum_{V_3} P_i^2 + \sum_{V_2} P_i^2 \tag{4.1}$$

For each position of the traverse, time signals are acquired from all microphones when the controller is on and off. The microphones are calibrated with a piston phone, and the Sound Pressure Level at each microphone is computed using the MATLAB PSD command [42].

*4.1.2 Comparison of Experimental and Simulation Results*

The results presented in Figure 4.2 have been obtained with a broad band disturbance signal between 40 and 250 Hz. As described in section 3.2, the velocity field of the disturbance plate was measured while the shaker was exciting it. The curves represent the 'pseudo' potential energy computed using data collected with the traverse. The curves obtained experimentally and with the model do not match although the global trends are the same. Global control (shown on both curves) was obtained on the entire frequency range, except in the 180-220 Hz frequency band. In fact, the model predicted very small attenuation in this band, but the actual experimental data showed that control was obtained, even though the reduction was low. In the rest of the band, the trends are very similar, even though the levels of attenuation are different. This can be explained by the fact that the model was developed in the frequency domain where actual causality problems in the design of the FIR filters of the controller were ignored. For this reason, it is normal for the model to predict more attenuation at each frequency. Nevertheless, the goal of the model was not to accurately predict the level of control achieved by the actual filtered-X LMS controller, but to provide an approximate shape of the control achievable by each configuration of actuators and sensors.

While Figures 4.2 (a) and (b) show the global control in the frequency domain, it was also of great importance to make sure that the actual spatial distribution of the attenuation, predicted by the model, was close to the attenuation measured in the test cavity. Figure 4.3 shows a schematic of the cavity with two planes. The horizontal plane is at the level of the ears of a person seated in the cavity, while the vertical plane is at the position of a supposed driver. In Figure 4.4 the results are presented for these two planes.

The acoustic modal analysis conducted in chapter 3 showed very good agreement between the model and the experiment, both in terms of natural frequencies and in terms of mode shapes. This proved that spatial distributions on resonance are very similar. This was also verified in Figure 4.4, where the attenuation obtained experimentally and with the finite element model at 120 Hz (on resonance) is shown. The shapes are very similar, even though more attenuation was obtained with the model towards the center of the cavity. While similar results were obtained for on-resonance frequencies, data, in the case of off-resonance frequencies, were

not as accurate when predicted by the model. Because the spatial distribution of the pressure field is much more complicated off-resonance than on-resonance (there are a lot of variations of the pressure in amplitude and phase in the off resonance case), the model requires more elements.

### *4.1.3 Conclusions*

Recalling that the goal of the model is its suitability for the development of a genetic algorithm to be used in the optimization of the locations of the actuators and sensors, the results are satisfactory for two reasons:

- The overall trends of the frequency responses, experimental and finite element model, are similar
- Spatial distribution is accurate on resonance.

Nevertheless, the limits of the model were reached off resonance. A good understanding of the system off resonance is not very important because the acoustic field is dominated by on resonance contents. Experimentally, the effects of the controller are predominant on resonance because it is where most of the energy of the system is concentrated.

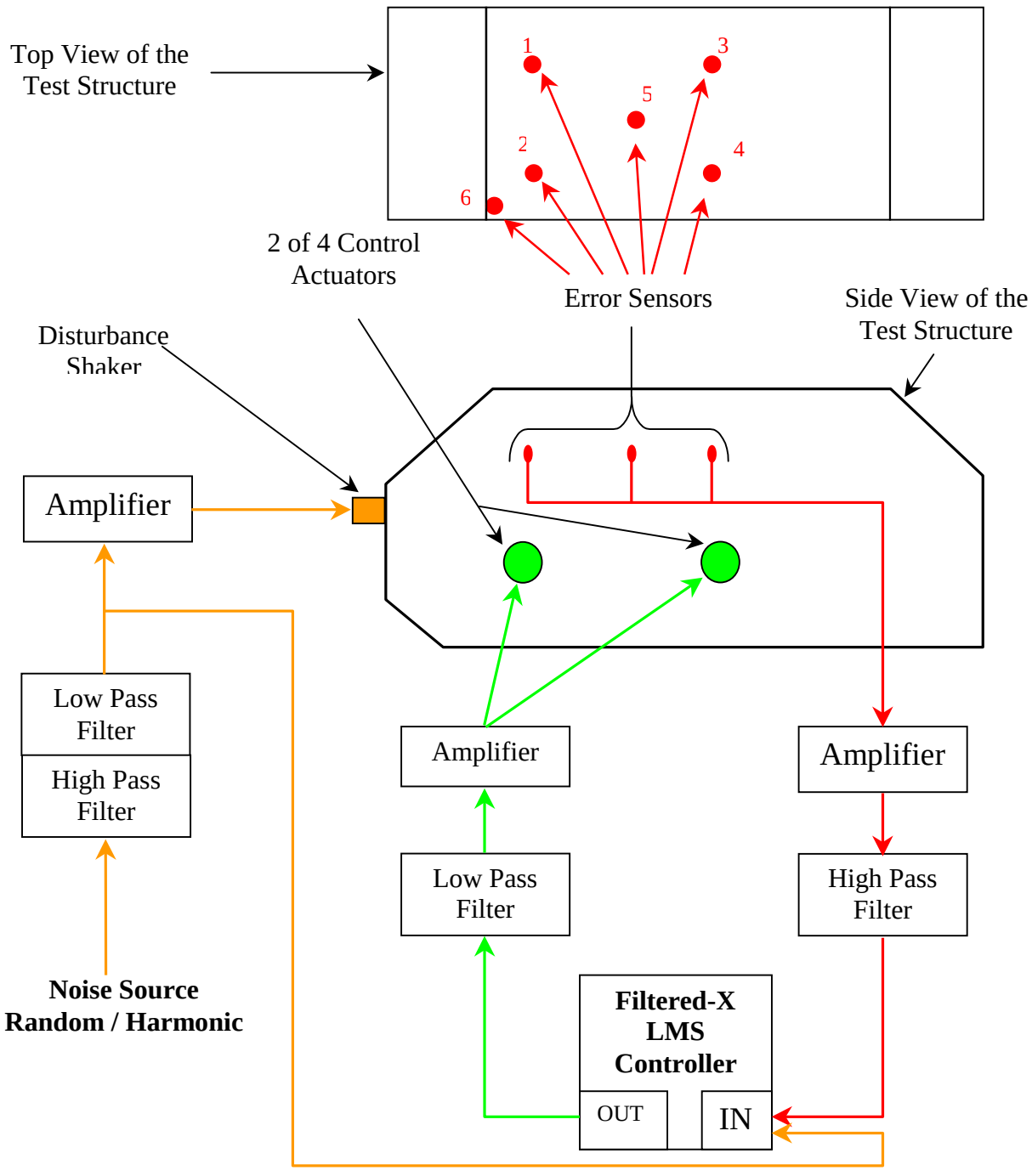


**Figure 4.1** Active noise control set-up in the test cavity

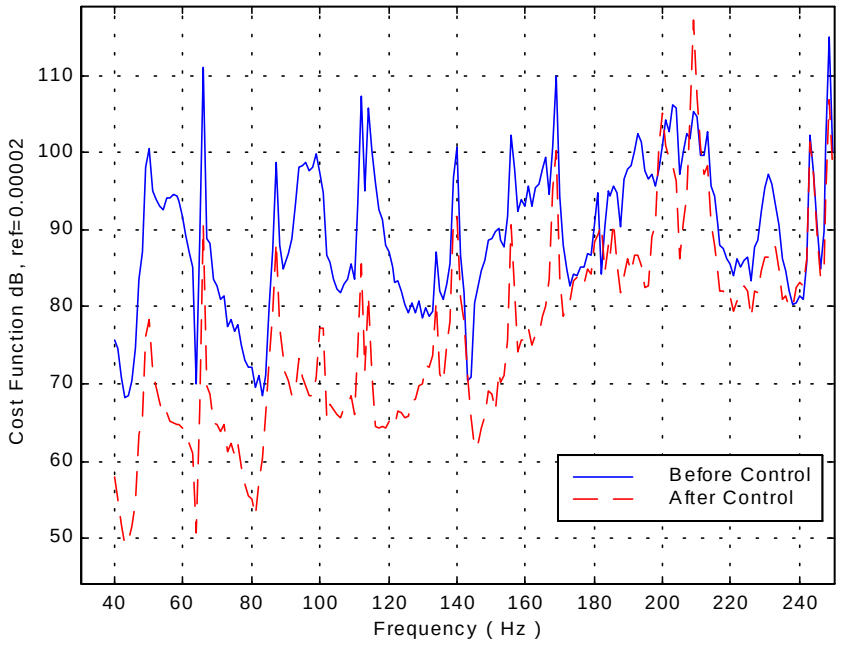


(a) Finite element model result

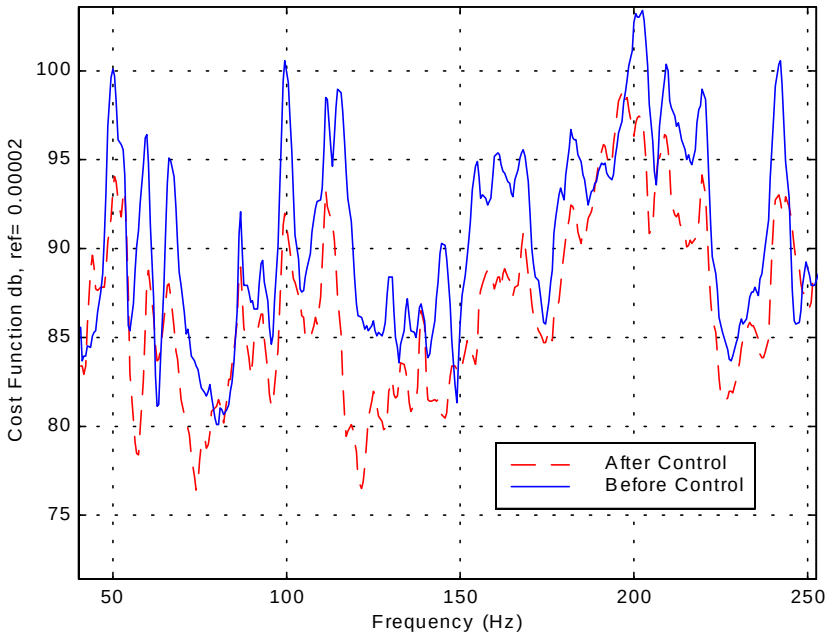


(b) Experimental result

**Figure 4.2** Frequency response - comparison of the model and the experiment

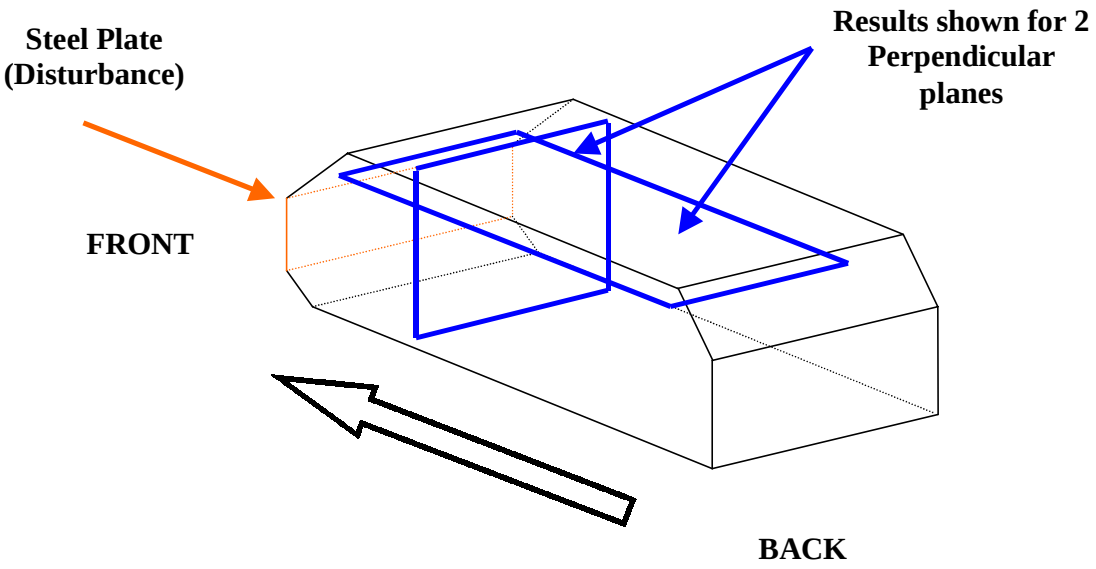


**Figure 4.3** Position of the two orthogonal planes used to show the results

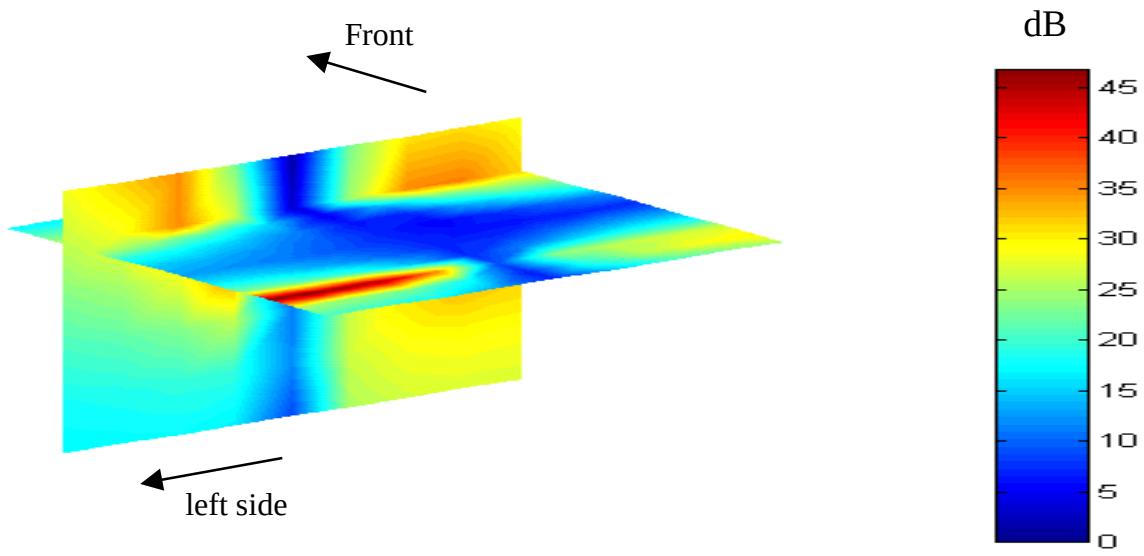


(a) Finite element model result

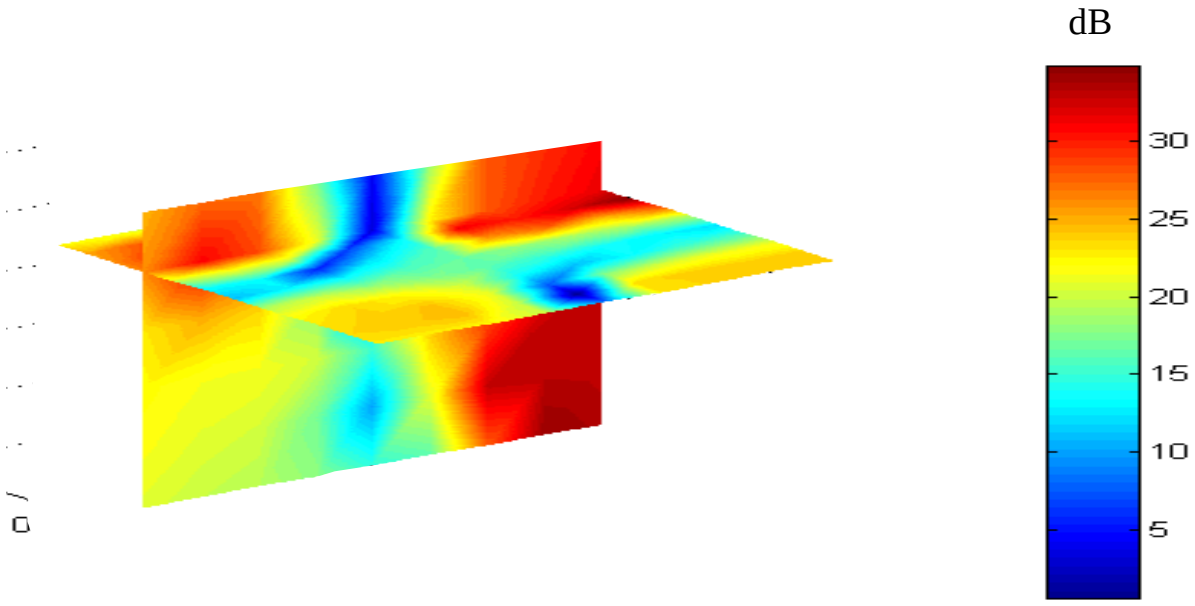


(b) Experimental result

**Figure 4.4** Spatial distribution of acoustic attenuation at 120 Hz (on resonance)

## 4.2 Application of the Genetic Algorithm

The principle of the genetic algorithm has been described in section 2.3. The goal of the genetic algorithm is to maximize a cost function, also called a fitness function, which characterizes the problem. The task proposed was to minimize the potential energy in the cavity between 40 and 250 Hz. The fitness has been computed as follows: in the first step, the 'pseudo' potential energy was computed for each frequency using the nodes of the finite element mesh corresponding to the traverse. In the second step, the total energy in the frequency band was computed by summing the values of the energy at each frequency. The fitness was the opposite of this value, hence, maximization of the fitness function led to an actual minimization of the energy. Two different fitness functions were used. In the first case, the summation over the frequencies was performed with data in dB. In the second configuration, the summation over the frequencies was performed with linear data. Results are shown in Figure 4.6.

The fitness function was computed for a certain combination of actuators and sensors, therefore candidate locations had to be chosen. Ideally, all the nodes of the mesh could be chosen as candidate sensor locations, and all the exterior surfaces chosen as candidate actuator locations. However, in the algorithm the parameters were coded as binary numbers, therefore, the number of candidate locations had to be a power of two. In the case of the sensors, all the nodes were candidate locations. There were 1848 nodes, and the nearest power of two was 2048. The algorithm was modified to ignore any combination of nodes including a location whose number lies between 1849 and 2048. In the case of the actuators, physical issues had to be taken into account. No actuators can be located in the windows or windshield. The total practical surface was well-described due to the placement of the sixty four locations (illustrated in Figure 4.5). Note that no candidate actuator was located in the trunk, to limit the algorithm to a reasonable domain of search.

The other parameters were chosen as follows:

- Crossover occurs with a probability of one.
- Mutation occurs with a probability of 3.3%, which corresponds to one member of each generation.
- The first generation was chosen randomly.
- The termination criteria was based on the fitness function. The algorithm was stopped when the difference between the average fitness of the generation at time n and the average fitness of the generation at time n-1 was less than 1%.

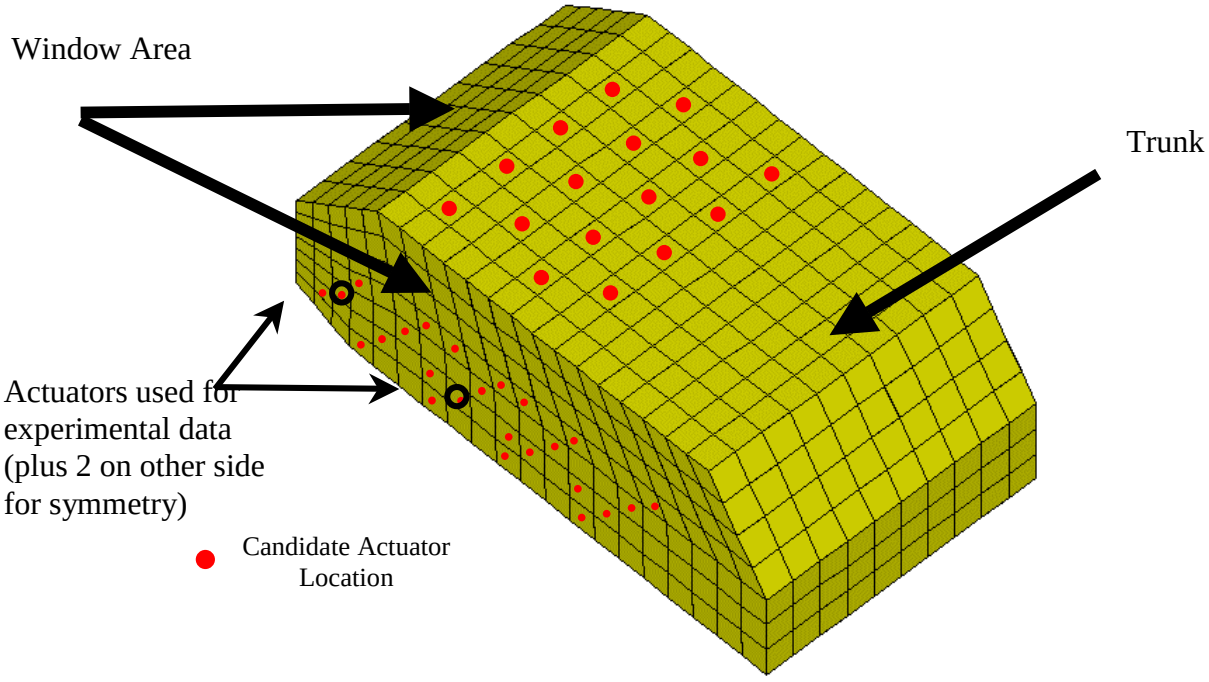


**Figure 4.5** Location of the candidate actuators

In the case of the first cost function (summation in dB), the algorithm converged after 27 iterations to a maximum fitness value of 8740. The frequency response obtained with the optimized configuration is shown in Figure 4.6 with a green line. In the case of the second cost function, the algorithm converged after 15 iterations, and the maximum fitness value was 998.9. The frequency response obtained with this optimized configuration is shown in Figure 4.6 with a magenta line. While the fitness value cannot be compared, it is interesting to compare the shapes of the frequency responses of the two optimized configurations.

The trends of the two curves are different. The second cost function (linear scale) leads to a flatter frequency response, which can be seen especially between 180 and 220Hz. On the other hand, between 80 and 150 Hz less attenuation is obtained than when the first cost function was used. This is clearly due to the effect of the logarithmic scale. In the case of a linear scale, the control is more concentrated at the frequencies where the levels are the highest (180-220 Hz).

In terms of actuator and sensor location, the results are very different also. This can be explained by the fact that the modes of importance are different for the two cost functions. Since the amplitude of the modes in the 180-220 Hz frequency band is higher, the second cost function tends to cancel those modes. In fact, the logarithmic scale diminishes the relative amplitude differences of the modes.

Results obtained with the optimization are compared with those obtained in the case where the actuators were located in each of the four doors and the sensors were located as illustrated in Figure 4.1. Using the first cost function, the fitness value was 8700 (8740 for the best configuration) and 997.4 using the second (998.9 for the best fitness). In terms of the fitness, only a negligible difference was obtained. Nevertheless, the frequency response is different from the response obtained with the two optimizations. Numerous fitness values that were close to the optimum were obtained with different configurations of actuators and sensors. Therefore numerous locations of actuators and sensors lead to similar attenuation in the 40 to 250 Hz frequency band. In fact, different frequency responses are obtained with each of these configurations, showing that a trade off has to be considered for broad band control. This implies that there is no ideal location for global control on all the frequencies.

Although good attenuation was obtained in numerous combinations there is a chance of getting poor results if the actuators and sensors are placed randomly (Figure 4.6). At some

frequencies, the effect of the control was negative and the total potential energy increased. Very little attenuation was obtained for other frequencies.

In conclusion, optimization by genetic algorithm was not very effective at finding an optimized set of actuators and sensors, since similar fitness values may be obtained with numerous different actuator and sensor configurations. Nevertheless, the genetic algorithm showed that:

- The second cost function was more effective in terms of global control in the frequency domain, since the frequency response, in the case of the optimum configuration, was flat.
- In some cases, the fitness value may drop drastically, proving the algorithm may be used to avoid poor configurations.
- The configuration used to develop the finite element model was close to optimum, therefore, this configuration was used for multiple harmonic tests as well as broad band tests.

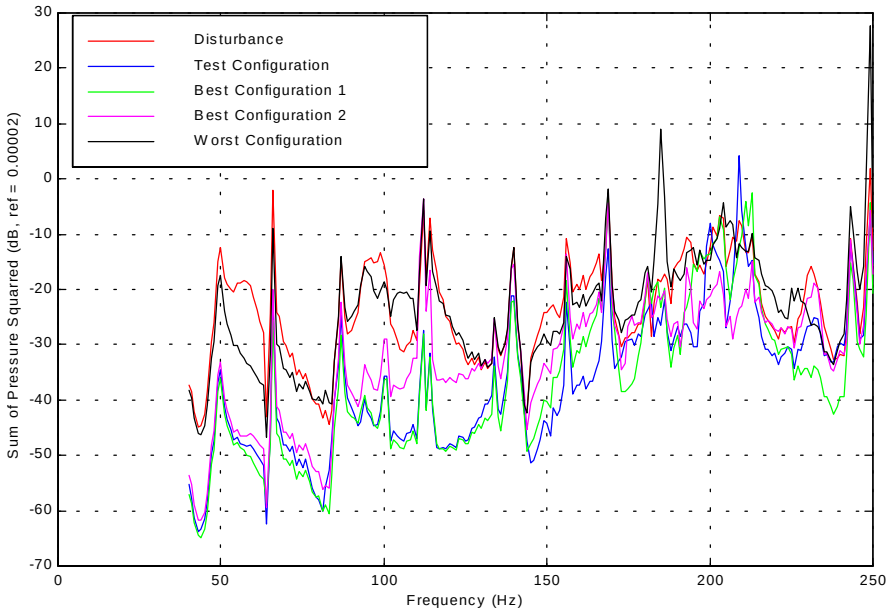


(a) Frequency response between 40 and 250 Hz

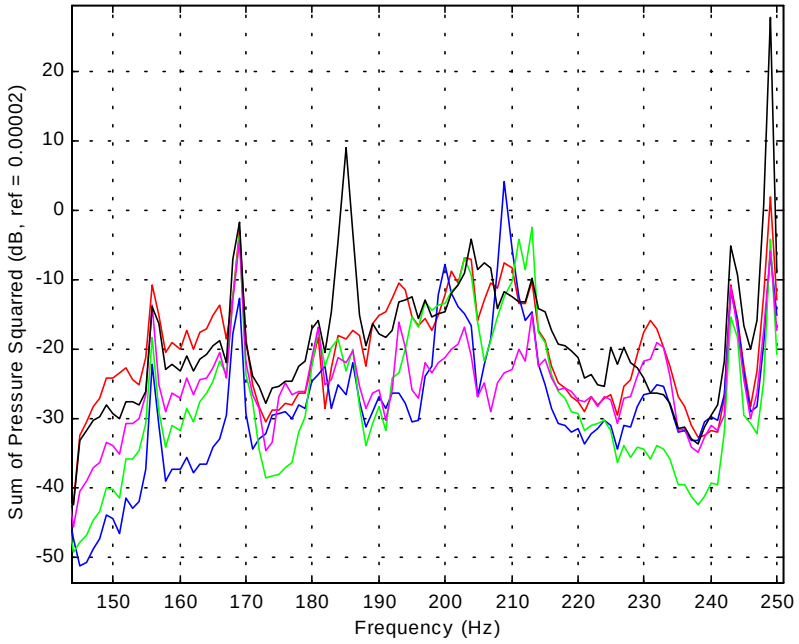


(b) Zoom between 150 and 250 Hz

**Figure 4.6** Results for different fitnesses

## 4.3 Experimental Active Noise Control Results with Optimized Configuration

According to the results obtained using the genetic algorithm on the model developed in chapter 3, there is no significant difference between the optimized set of actuators and sensors and the configuration used to validate the model (described in Figure 4.1). For this reason, an extensive study of the active noise control system was performed using the latter configuration. The control was applied to two types of disturbances, harmonic and broad band.

### *4.3.1 Application in the Case of a Harmonic Disturbance*

Harmonic control was performed for eight different frequencies from 80 to 310 Hz. The results obtained are shown in Table 4.1. For each frequency, results include sound pressure level (before and after control) attenuation at each of the six error sensors, and the total reduction computed using the microphones located on the traverse. Global attenuation is also plotted in a bar graph in Figure 4.7. Global attenuation was computed in two steps. First, for both the cases before and after control, the pressure squared at the sensors are summed up. Second, the logarithmic value of their ratio is obtained and multiplied by ten to obtain a value in decibel.

In order to study the effect of control, each of the chosen frequencies had different modal characteristics which can be classified as follows:

- Off resonance case, at 80 Hz, 145 Hz and 305 Hz
- On resonance case
    - 1 Mode, at 100 Hz and 310 Hz.
    - 2 Modes, at 118 Hz
    - high modal density, at 184 Hz and 210 Hz

On resonance, high global attenuation was achieved. The level of the attenuation was 9.8 dB at 310 Hz, while the attenuation at lower frequencies was higher, 13.9 dB at 100 Hz and 18.5 dB at 118 Hz. The spatial distribution of the Sound Pressure Level, before and after control, is shown in Figures 4.8, 4.9 and 4.10 for 100 Hz, 118 Hz and 145 Hz, respectively. For the three

cases, the level, before and after control, is shown together with the attenuation for two orthogonal planes. The position of these two planes relative to the rest of the structure is shown in Figure 4.3. For these three frequencies, the effect of the control was spatial averaging. Reduction of the sound pressure level (SPL) was obtained where the pressure level was high before control (anti-nodes); however, the SPL was raised where it was low (nodes). For this reason, the attenuation plot is similar to the mode shape at 100 Hz, and the pressure before control at 118 Hz. The pressure is the superposition of two modes occurring at the same frequency.

For the other cases, occurring either off resonance or at frequencies where the modal density is high, the control is not effective. The global control is less than 6.3 dB and drops as low as 0.5 dB at 80Hz. An exception is made at 145 Hz, where the global attenuation is 14.6 dB. As shown in Table 4.1, the control is only local for all these frequencies. For example, at 80 Hz, attenuation of 23.5 dB and 19.9 dB was achieved at error microphones five and six respectively. The number of modes that contribute to the response at off-resonance frequencies is very high. In general, a system with n degrees of freedom can be controlled by n inputs. In the case of a continuous system, as it is described here, the number of degrees of freedom is frequency dependent and is equal to the number of modes that significantly contribute to the response at that frequency. This number of modes is typically high for off-resonance frequencies. Therefore, global control is not achievable with a low number of control sources. Note in the case where the disturbance is at 145 Hz, global attenuation of 14.5 dB was achieved. This is due to the three modes being within a 60 Hz band around 145 Hz (154, 159 and 165 Hz). Thus by definition, in the case of high modal density, the number of degrees of freedom is high, and therefore, it was predictable that only little control would be achieved.

It can be concluded that the performance of global control in a cavity depends on the number of modes that contribute to the response at a particular frequency. Typically, many modes have to be included in an off-resonance analysis or when a high density of modes is being considered. The harmonic results that have been discussed show that very little attenuation was achieved using four actuators at frequencies with high modal density (6.3 dB at 184 Hz and 2.5 dB at 210 Hz), as well as off-resonance frequencies (0.5 dB at 80 Hz and 1.7 dB at 305 Hz). An exception is made for the case at 145 Hz, where attenuation of 14.6 dB is achieved. On the other

hand, when the response is highly dominated by one to three modes the attenuation is very good (more than 14 dB).

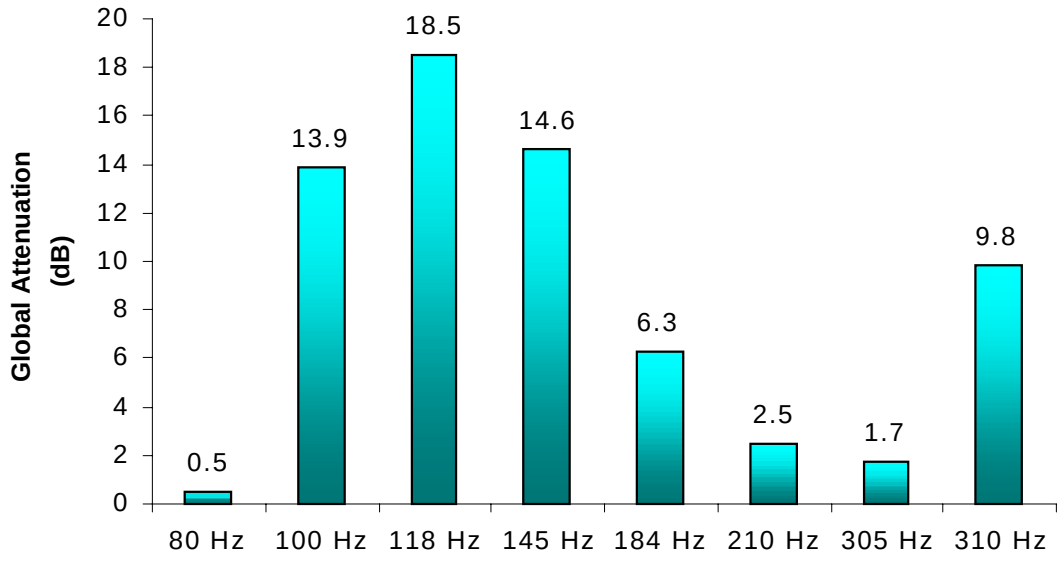


**Figure 4.7** Attenuation measured for harmonic control

**Table 4.1** Control results at obtained with an harmonic disturbance

| **Frequency** | | **Total** | **Error 1** | **Error 2** | **Error 3** | **Error 4** | **Error 5** | **Error 6** |
|---|---|---|---|---|---|---|---|---|
| 80 Hz | SPL B. C.[1] | 109.2 | 103.5 | 99.7 | 98.9 | 103.1 | 112.3 | 114.9 |
| | SPL A. C.[2] | 108.7 | 97.5 | 95.9 | 94 | 102.1 | 88.8 | 95 |
| | **Attenuation (dB)** | **0.5** | **6** | **3.8** | **4.9** | **1** | **23.5** | **19.9** |
| 100 Hz | SPL B. C.[1] | 123.6 | 98.5 | 97.3 | 97.9 | 80.2 | 97.5 | 99.1 |
| | SPL A. C.[2] | 109.7 | 78.3 | 77.1 | 73.9 | 76.6 | 70.6 | 82.3 |
| | **Attenuation (dB)** | **13.9** | **20.2** | **20.2** | **24** | **3.6** | **26.9** | **16.8** |
| 118 Hz | SPL B. C.[1] | 126.4 | 104.3 | 99.1 | 101.9 | 96.2 | 101.6 | 89.6 |
| | SPL A. C.[2] | 107.9 | 75.4 | 81.7 | 75.9 | 84 | 78.2 | 71.6 |
| | **Attenuation (dB)** | **18.5** | **28.9** | **17.4** | **26** | **12.2** | **23.4** | **18** |
| 145 Hz | SPL B. C.[1] | 120.6 | 93.8 | 96.6 | 87.2 | 89.3 | 90.2 | 95.8 |
| | SPL A. C.[2] | 106 | 78.7 | 73.6 | 66 | 78.4 | 76.2 | 72 |
| | **Attenuation (dB)** | **14.6** | **15.1** | **23** | **21.1** | **10.9** | **14** | **23.8** |
| 184 Hz | SPL B. C.[1] | 120.8 | 100.8 | 94.1 | 101.7 | 85.8 | 101.7 | 88.8 |
| | SPL A. C.[2] | 114.5 | 79.1 | 90.2 | 76.5 | 83.2 | 78.7 | 83.6 |
| | **Attenuation (dB)** | **6.3** | **21.7** | **3.9** | **25.2** | **2.6** | **23** | **5.2** |
| 210 Hz | SPL B. C.[1] | 120.5 | 94.9 | 92.4 | 75.2 | 94.5 | 91.1 | 87.8 |
| | SPL A. C.[2] | 118 | 75.8 | 88 | 80.3 | 78 | 89.6 | 82.4 |
| | **Attenuation (dB)** | **2.5** | **19.1** | **4.4** | **-5.1** | **16.5** | **1.5** | **5.4** |
| 305 Hz | SPL B. C.[1] | 118.2 | 89.9 | 86.2 | 76.2 | 94.1 | 84.4 | 92.3 |
| | SPL A. C.[2] | 116.5 | 73.8 | 81.5 | 84.2 | 77 | 81.3 | 78.6 |
| | **Attenuation (dB)** | **1.7** | **16.1** | **4.7** | **-8** | **17.1** | **3.1** | **13.7** |
| 310 Hz | SPL B. C.[1] | 123.5 | 97.3 | 100.9 | 91.6 | 92.9 | 90.3 | 99.4 |
| | SPL A. C.[2] | 113.7 | 78.7 | 73.6 | 84.9 | 78.1 | 79.9 | 78.1 |
| | **Attenuation (dB)** | **9.8** | **18.6** | **27.3** | **6.7** | **14.8** | **10.4** | **21.3** |

[1] Sound Pressure Level in decibel Before Control

[2] Sound Pressure Level in decibel After Control

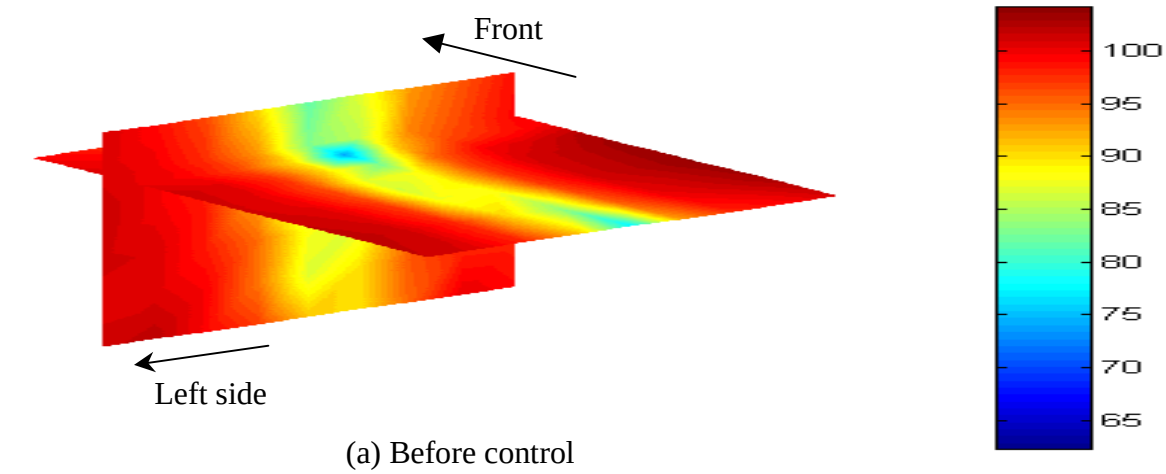


(a) Before control

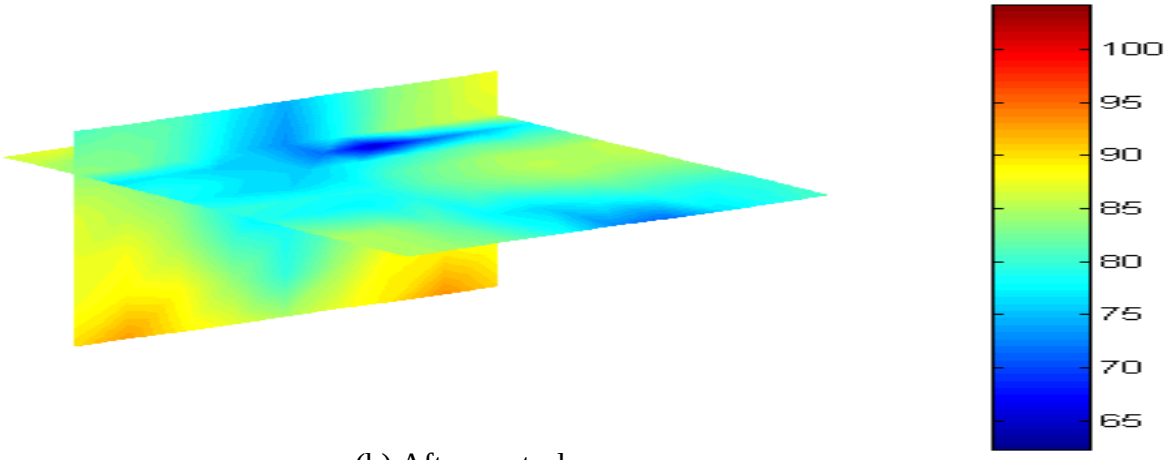


(b) After control

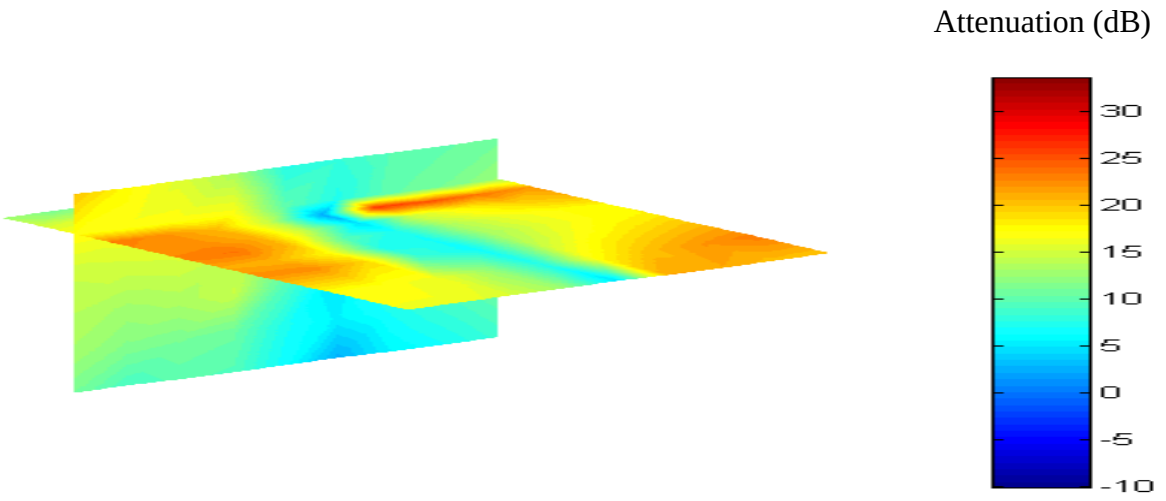


(c) Attenuation

**Figure 4.8** Sound pressure level at 100 Hz

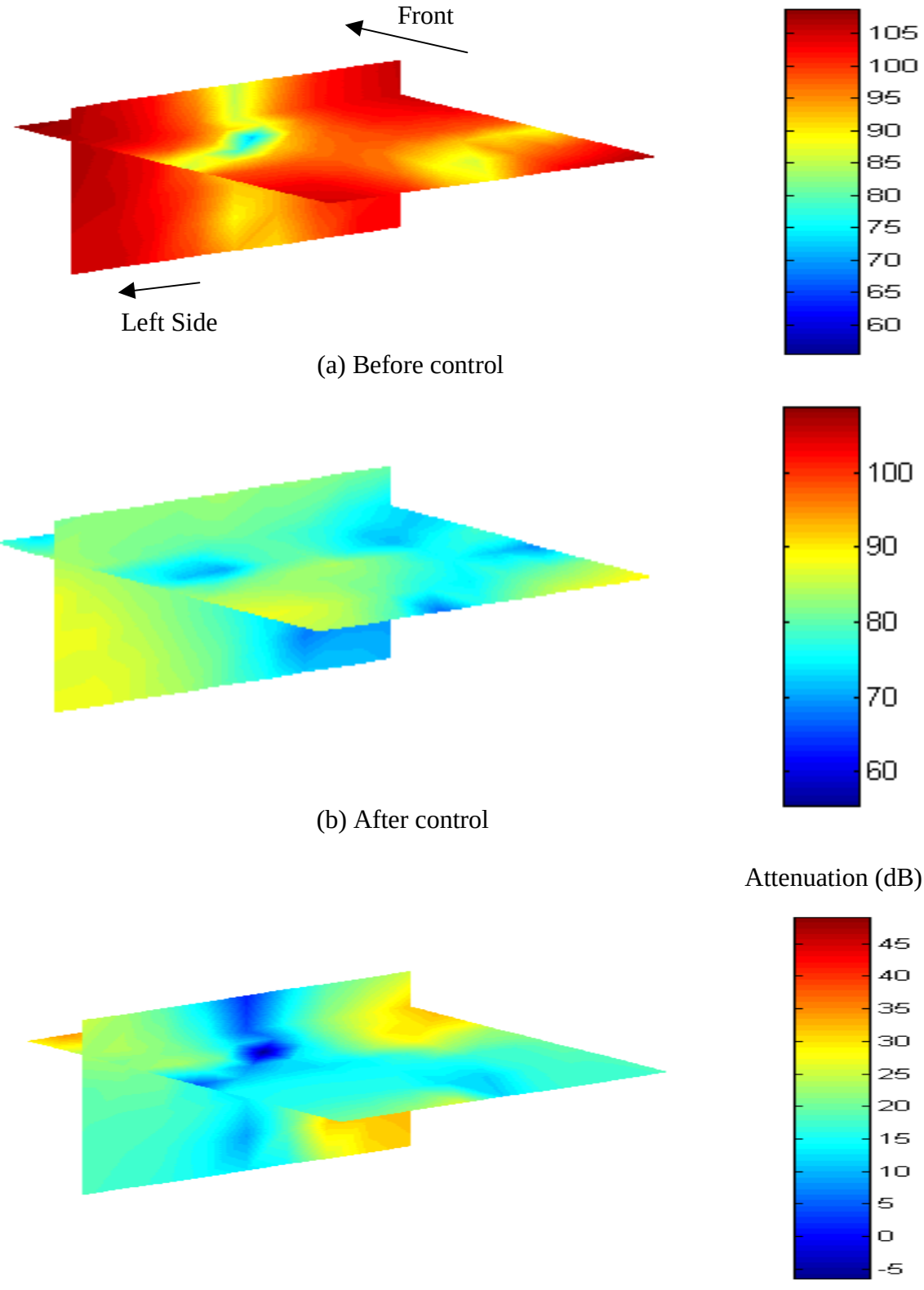


(a) Before control

(b) After control

(c) Attenuation

**Figure 4.9** Sound pressure level at 118 Hz

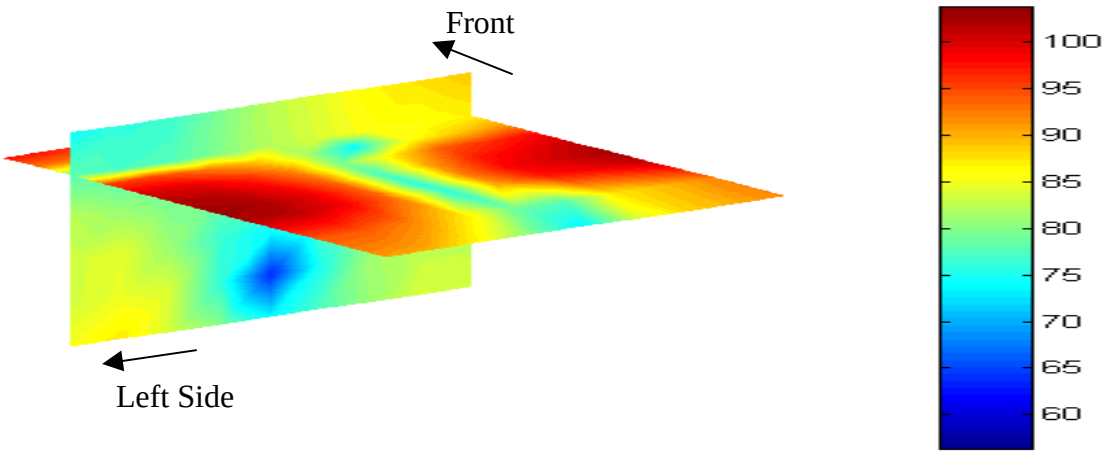


(a) Before control

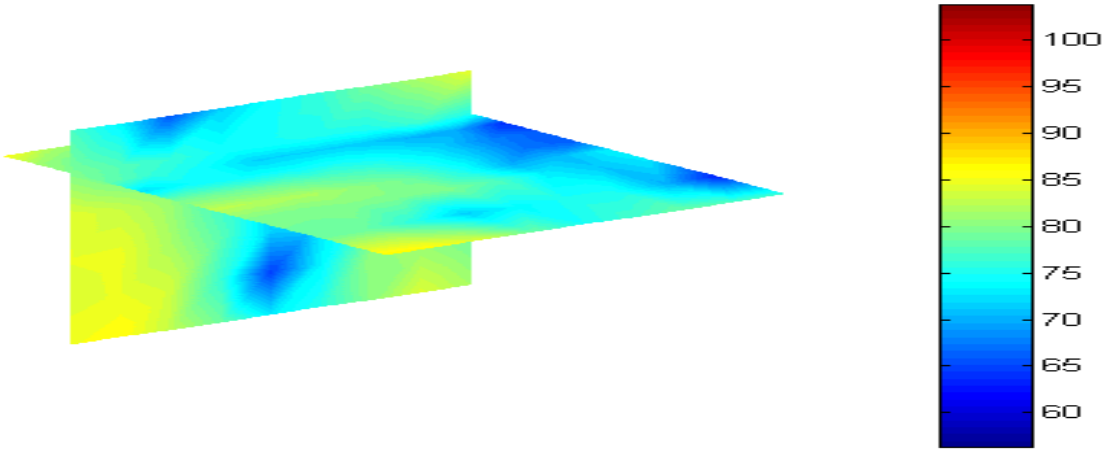


(b) After control

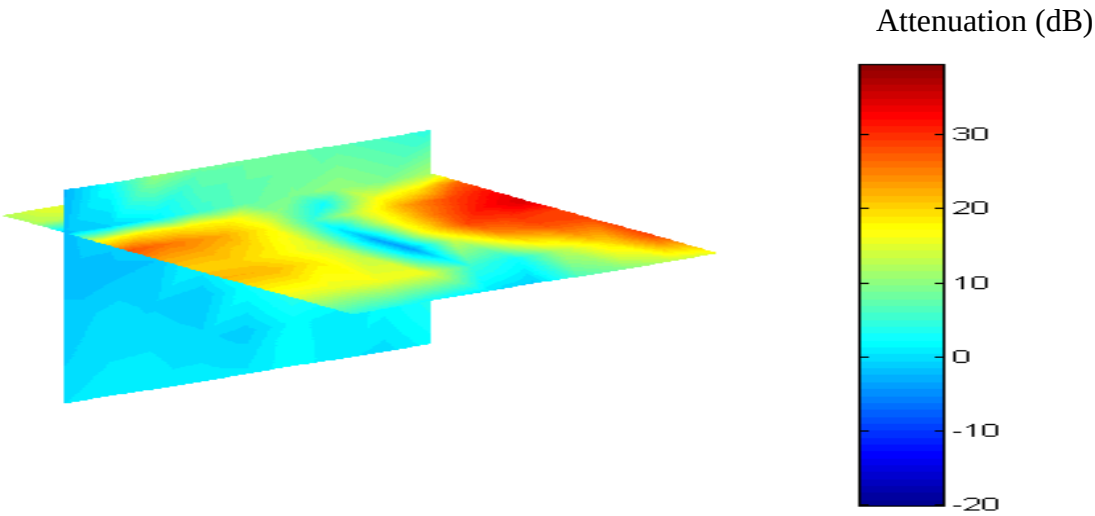


(c) Attenuation

**Figure 4.10** Sound pressure level at 145 Hz

*4.3.2 Active Noise Control Results when the Disturbance is a Broad Band Signal*

Road noise and power train noise are broad band disturbances, because the acoustic energy measured inside the cabin of an automobile is spread over a wide frequency band. The characteristics of these two types of noise will be discussed in detail in chapter 5. Harmonic tests give insight into the performance achievable, frequency by frequency, by the controller. In this chapter, results are shown for the case of optimum location for four actuators and six error sensors. Results obtained with a system using only four error sensors are also presented. The set-up used for the control is the same as previously described in Figure 4.1.

The critical point during the design of a broad band control system is the choice of digital filters to be used in the controller (for both the system identification and the control paths), as well as the number of coefficients to include in each filter. Finite Impulse Response filters were used for both the system identification and the control. The number of coefficients was limited by the computation capabilities of the computer. Lowering the number of error sensors increases the number of coefficients that might be used in each filter. In a four by six system with one reference, the number of filters is twenty-four for the system identification and four for the control. For a four by four system, only sixteen system ID filters are required. In this last case, it was possible to increase the maximum number of coefficients per filter.

In the case of the system including six error sensors, 120 coefficients were used for the system identification and 180 coefficients were used for the control. In the case of the system including four error sensors, 120 coefficients were used for the system identification while 300 were used for the control. The identification of the transfer functions (System ID) showed good results with filters having 120 coefficients. Therefore, no coefficients were added to the system ID filters in the configuration involving four error sensors. Coefficients were added to the control filters in order to achieve more control at the error sensors. The attenuation of the sound pressure level in the cavity obtained with the two systems is presented in Table 4.2.

The effects of the control are different in the two systems (system 1 has four error sensors and system 2 has six error sensors). With system 1, higher reduction was obtained at the error sensors, as illustrated in Table 4.2. This is due to two factors. First, because the system is fully-determined, a theoretically minimum exists at zero for the sum of the pressure squared at the

error sensors. In an over determined system, the minimum is higher than zero. Second, because more coefficients are used in the control filters, the control path model is more accurate. A typical frequency response at an error sensor is shown, for the two systems, in Figures 4.11 and 4.12. Note that the general shapes are similar. The control cancels all the resonance peaks with a maximum peak reduction of 25 dB, and the frequency responses are more flat. For this reason, attenuation above 250 Hz is low, since the level before control was low. However, the total reduction in the 40-400 Hz band is 2 dB higher in the case of system 1 at each error sensor.

In terms of global reduction, the total reduction in the frequency band is close to 4 dB for the two systems. Figures 4.13 and 4.14 show the spectrum at the sensors mounted on the traverse (the sum of the pressure squared at each frequency) for the four by six and four by four systems, respectively. In both cases, little reduction is obtained above 250 Hz, while all the peaks are cancelled at lower frequencies. The most important difference between the two systems is the spatial distribution of the sound pressure level after control. In the case of the fully determined system, the control is more localized around the error sensors (Figure 4.16). Four zones of quiet are clearly marked at these locations. The same effect is not visible in the case of the over determined system. Although the reduction is lower at the error sensors, the control is much more global, as illustrated in Figure 4.15.

**Table 4.2** Results obtained with a broad band disturbance

| **Control System dimensions** | **Global** | **Error 1** | **Error 2** | **Error 3** | **Error 4** | **Error 5** | **Error 6** |
|---|---|---|---|---|---|---|---|
| **4 by 4** Control on | | 81.4 | 81.1 | 80.8 | 82.4 | / | / |
| Control off | | 94.2 | 93.7 | 91.4 | 92.3 | / | / |
| **Attenuation** | **3.8** | 12.8 | 12.6 | 10.6 | 9.9 | / | / |
| **4 by 6** Control on | | 87.8 | 84.9 | 85.7 | 85.5 | 83.7 | 84.6 |
| Control off | | 98.5 | 93.4 | 93.8 | 91.8 | 91.8 | 90.9 |
| **Attenuation** | **3.8** | 10.7 | 8.5 | 8.1 | 6.3 | 8.1 | 6.3 |

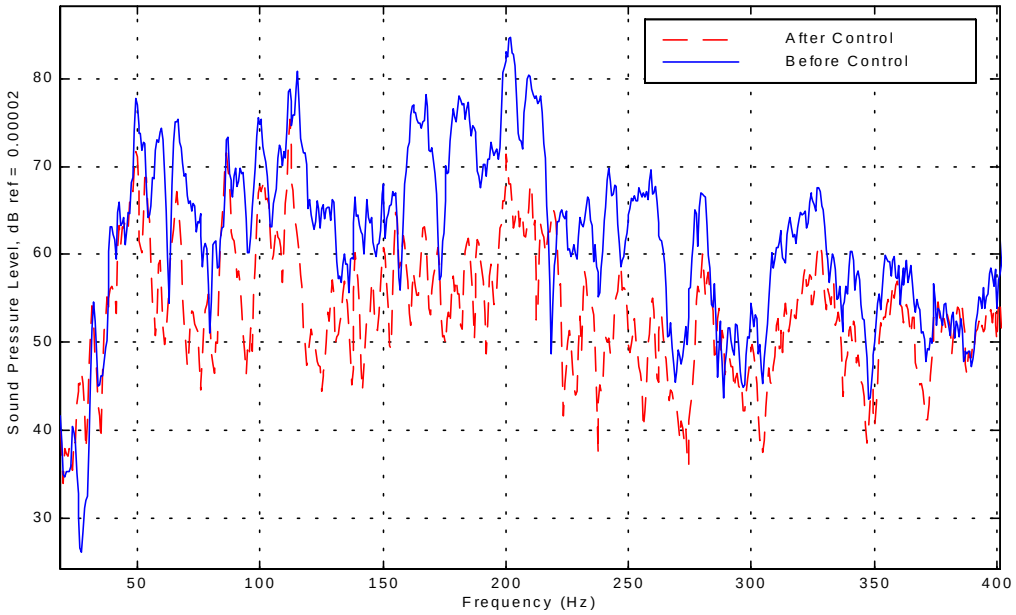


**Figure 4.11** Signal at error sensor 1 (four by six system)

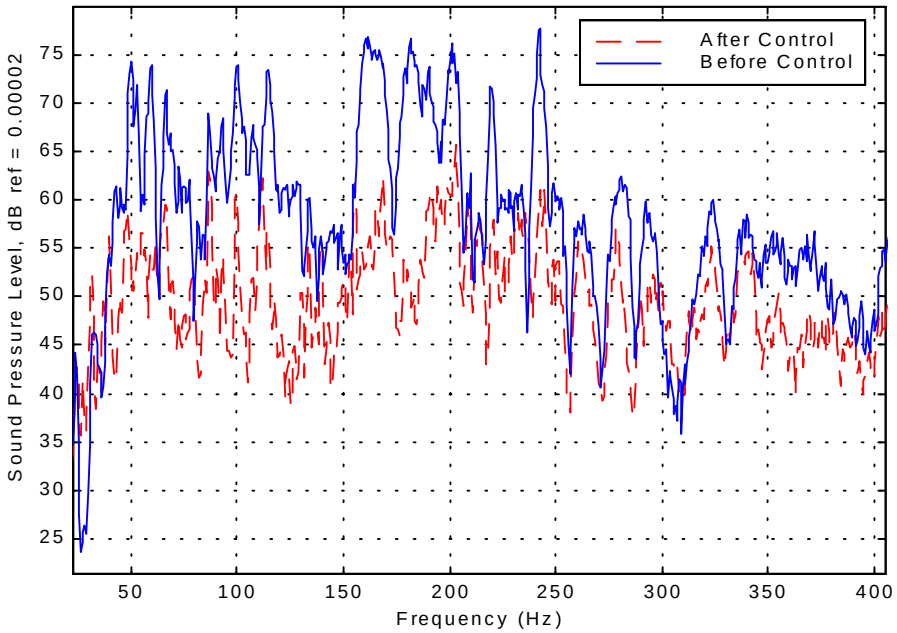


**Figure 4.12** Signal at error sensor 1 (four by four system)

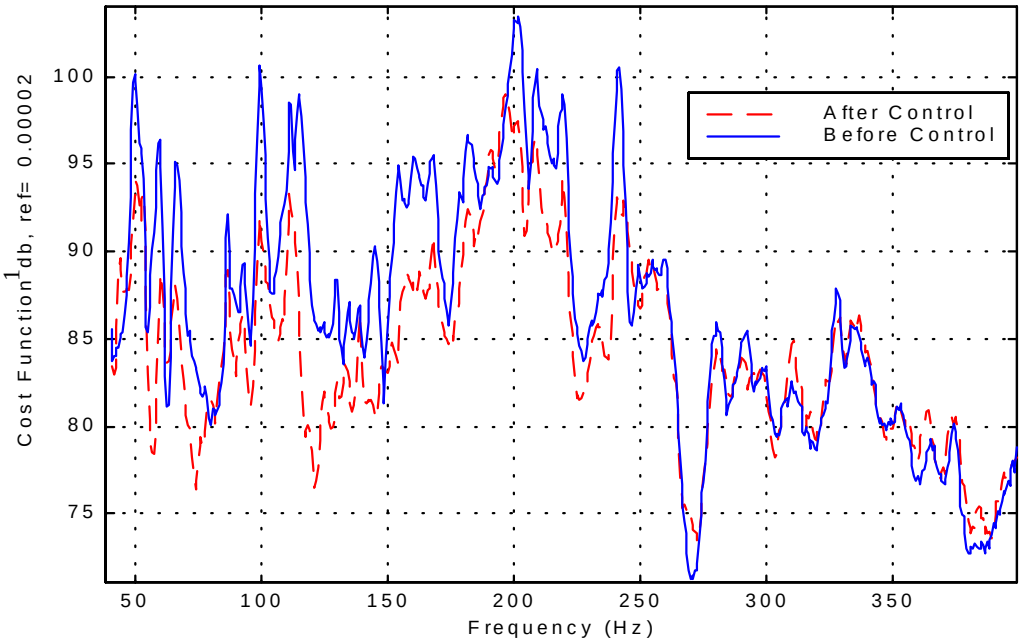


**Figure 4.13** Global control; four by six system

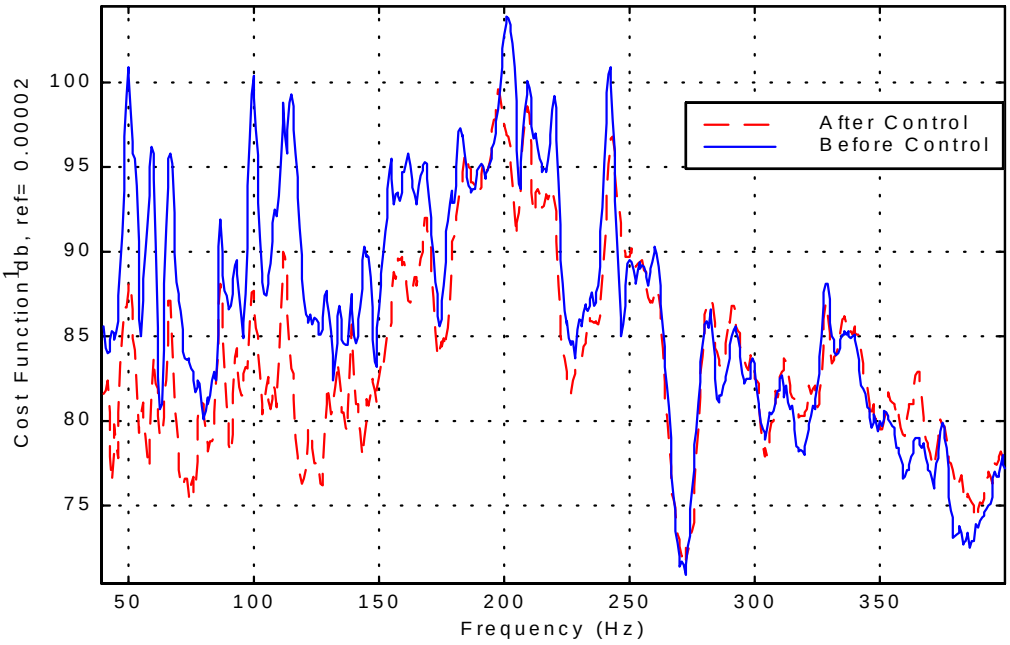


**Figure 4.14** Global control; four by four system

[1] the cost function is defined for each frequency as the sum of the pressure squared at each of the microphones mounted on the grid

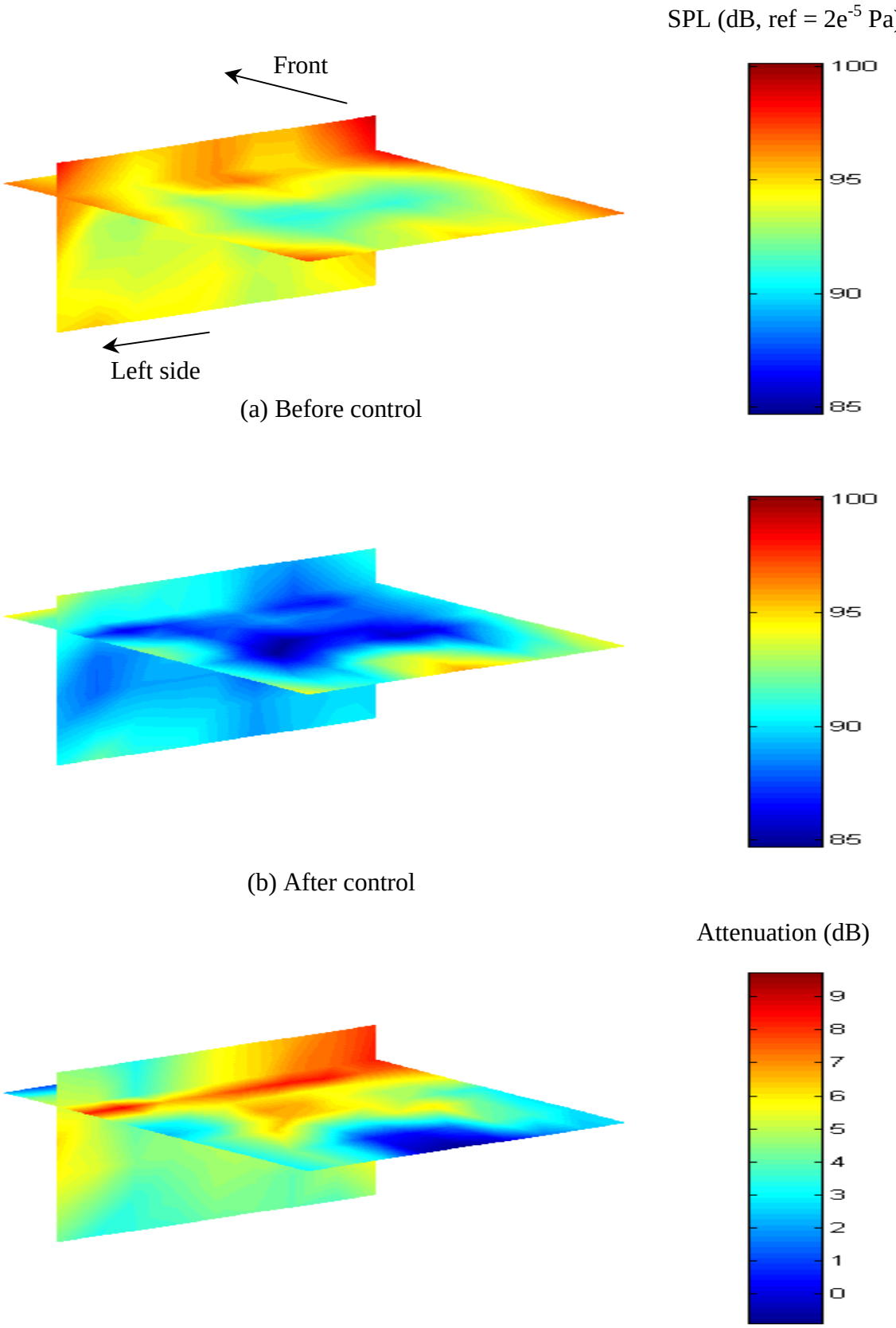


(a) Before control

(b) After control

(c) Attenuation

**Figure 4.15** Sound pressure level 40-500 Hz; four by six system

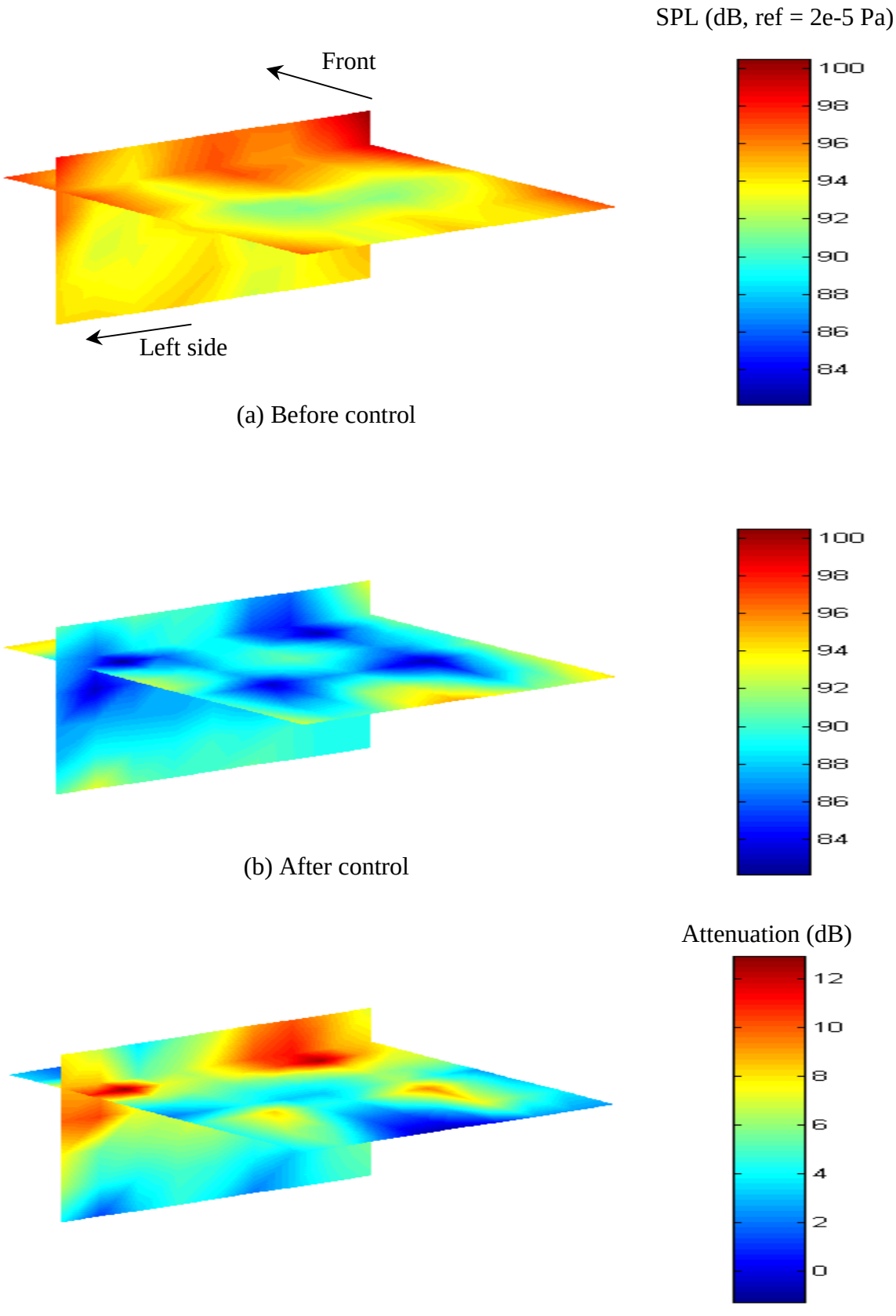


(a) Before control

(b) After control

(c) Attenuation

**Figure 4.16** Sound pressure level 40-500 Hz; four by four system

### *4.3.3 Conclusions*

From the experiments conducted on the test cavity system, conclusions can be drawn and applied to the control of disturbances, both harmonic and broad band, in a three-dimensional cavity like an automobile.

First, it was shown that using four secondary sources, global control was efficient at frequencies where the response was dominated by less than four modes. Only four degrees of freedom can be globally controlled with four control sources.

Second, cancellation of the modes suppresses the peaks of the frequency response, such that the response after control is relatively flat. The implication is that the ultimate attenuation of the sound pressure levels depends on the damping of the modes (i.e. sharpness of the peaks).

Third, global control was achieved with both a fully-determined and over-determined system. However, a fully-determined system leads to the appearance of zones of quiet around the error sensors. With an over determined system, attenuation at the error sensors is lower, but the control is more global.

In an automobile, the attenuation of the sound pressure will depend on the dynamics of the cabin. If the damping is high, a large number of control sources will be required to achieve global control of the sound pressure. As it was discussed in section 4.2, the locations of the control sources do not affect global control. Therefore, the location of the pre-existing speakers was chosen. In order to create a zone of quiet around the head of the passengers and driver at frequencies where no global control is achievable, the error sensors would have to be located close to the ears of the driver and passengers. A detailed discussion of the control parameters (locations of the reference sensors, control sources and error sensors, as well as the signal processing) will be discussed in chapter 5.